



## Molecular determinants and intracellular targets of taurine signalling in pancreatic islet $\beta$ -cells

Turbitt, J., Moffett, R. C., Brennan, L., Johnson, P. R. V., Flatt, P. R., McClenaghan, N. H., & Tarasov, A. I. (2024). Molecular determinants and intracellular targets of taurine signalling in pancreatic islet  $\beta$ -cells. *Acta Physiologica*, Article e14101. Advance online publication. <https://doi.org/10.1111/apha.14101>

[Link to publication record in Ulster University Research Portal](#)

**Published in:**  
Acta Physiologica

**Publication Status:**  
Published online: 20/01/2024

**DOI:**  
[10.1111/apha.14101](https://doi.org/10.1111/apha.14101)

**Document Version**  
Publisher's PDF, also known as Version of record

**General rights**  
Copyright for the publications made accessible via Ulster University's Research Portal is retained by the author(s) and / or other copyright owners and it is a condition of accessing these publications that users recognise and abide by the legal requirements associated with these rights.

**Take down policy**  
The Research Portal is Ulster University's institutional repository that provides access to Ulster's research outputs. Every effort has been made to ensure that content in the Research Portal does not infringe any person's rights, or applicable UK laws. If you discover content in the Research Portal that you believe breaches copyright or violates any law, please contact [pure-support@ulster.ac.uk](mailto:pure-support@ulster.ac.uk).

## RESEARCH PAPER

# Molecular determinants and intracellular targets of taurine signalling in pancreatic islet $\beta$ -cells

Julie Turbitt<sup>1</sup> | R. Charlotte Moffett<sup>1</sup>  | Lorraine Brennan<sup>2,3</sup>  | Paul R. V. Johnson<sup>4,5</sup> | Peter R. Flatt<sup>1</sup>  | Neville H. McClenaghan<sup>1,6</sup>  | Andrei I. Tarasov<sup>1</sup> 

<sup>1</sup>School of Biomedical Sciences, Ulster University, Coleraine, UK

<sup>2</sup>UCD Institute of Food and Health, UCD School of Agriculture and Food Science, University College Dublin, Dublin 4, Republic of Ireland

<sup>3</sup>UCD Conway Institute of Biomolecular and Biomedical Research, University College Dublin, Dublin 4, Republic of Ireland

<sup>4</sup>Nuffield Department of Surgical Sciences, Oxford Centre for Diabetes, Endocrinology and Metabolism, University of Oxford, Churchill Hospital, Oxford, UK

<sup>5</sup>Oxford Biomedical Research Centre (OxBRC), Oxford, UK

<sup>6</sup>Department of Life Sciences, Atlantic Technological University, Sligo, Republic of Ireland

## Correspondence

Neville H. McClenaghan and Andrei I. Tarasov, School of Biomedical Sciences, Ulster University, Cromore Road, Coleraine BT52 1SA, UK.  
Email: [neville.mcclenaghan@atu.ie](mailto:neville.mcclenaghan@atu.ie) and [a.tarasov@ulster.ac.uk](mailto:a.tarasov@ulster.ac.uk)

## Funding information

Research and Development Office of the Northern Ireland Department for Health and Personal Social Services; University of Ulster Research strategy funding; Diabetes UK

## Abstract

**Aim:** Despite its abundance in pancreatic islets of Langerhans and proven antihyperglycemic effects, the impact of the essential amino acid, taurine, on islet  $\beta$ -cell biology has not yet received due consideration, which prompted the current studies exploring the molecular selectivity of taurine import into  $\beta$ -cells and its acute and chronic intracellular interactions.

**Methods:** The molecular aspects of taurine transport were probed by exposing the clonal pancreatic BRIN BD11  $\beta$ -cells and primary mouse and human islets to a range of the homologs of the amino acid (assayed at 2–20 mM), using the hormone release and imaging of intracellular signals as surrogate read-outs. Known secretagogues were employed to profile the interaction of taurine with acute and chronic intracellular signals.

**Results:** Taurine transporter TauT was expressed in the islet  $\beta$ -cells, with the transport of taurine and homologs having a weak sulfonate specificity but significant sensitivity to the molecular weight of the transporter. Taurine, hypotaurine, homotaurine, and  $\beta$ -alanine enhanced insulin secretion in a glucose-dependent manner, an action potentiated by cytosolic  $\text{Ca}^{2+}$  and cAMP. Acute and chronic  $\beta$ -cell insulinotropic effects of taurine were highly sensitive to co-agonism with GLP-1, forskolin, tolbutamide, and membrane depolarization, with an unanticipated indifference to the activation of PKC and CCK8 receptors. Pre-culturing with GLP-1 or  $\text{K}_{\text{ATP}}$  channel inhibitors sensitized or, respectively, desensitized  $\beta$ -cells to the acute taurine stimulus.

**Conclusion:** Together, these data demonstrate the pathways whereby taurine exhibits a range of beneficial effects on insulin secretion and  $\beta$ -cell function, consistent with the antidiabetic potential of its dietary low-dose supplementation.

## KEYWORDS

$\text{Ca}^{2+}$  dynamics, cell signalling, insulin secretion, taurine homologs, taurine transport

This is an open access article under the terms of the [Creative Commons Attribution-NonCommercial](https://creativecommons.org/licenses/by-nc/4.0/) License, which permits use, distribution and reproduction in any medium, provided the original work is properly cited and is not used for commercial purposes.

© 2024 The Authors. *Acta Physiologica* published by John Wiley & Sons Ltd on behalf of Scandinavian Physiological Society.

## 1 | INTRODUCTION

Alongside glucose, amino acids represent a major class of physiological nutrient regulators of insulin secretion.<sup>1–3</sup> There is no unique mechanism whereby the diverse range of essential and non-essential amino acids impacts the secretory output of pancreatic  $\beta$ -cells,<sup>4–7</sup> with the timescale of the reported effects ranging from minutes<sup>8</sup> to days.<sup>9</sup> Thus, the acute insulinotropic<sup>10,11</sup> and antihyperglycemic<sup>12</sup> effects of the sulfur-containing amino acid taurine, highly abundant in pancreatic islets,<sup>13</sup> are mediated by the elevation of cytosolic  $\text{Ca}^{2+}$  levels ( $[\text{Ca}^{2+}]_{\text{cyl}}$ ) in  $\beta$ -cells.<sup>9</sup> The specificity of the effect is, nevertheless, unclear, as it is linked to the transport of the amino acid into the  $\beta$ -cell, presumably via the high-affinity taurine transporter TauT that has a broad ligand repertoire.<sup>14</sup> Likewise unclear is the link of the  $\text{Ca}^{2+}$  dynamics on the balance between oxidative metabolism and anaplerosis, which is controlled by taurine on a longer timescale.<sup>8</sup> Although the oxidative metabolism couples the glucose stimulus to the inhibition of ATP-sensitive  $\text{K}^+$  ( $\text{K}_{\text{ATP}}$ ) channels,<sup>15</sup> the replenishment of the pool of the TCA cycle metabolites via anaplerosis is considered a bottleneck of the metabolic signalling in  $\beta$ -cells,<sup>16</sup> conventionally ascribed to the second, “amplifying”<sup>17</sup> stages of glucose-induced insulin secretion.<sup>18</sup> The mechanistic link between taurine stimulus and the anaplerotic response, which progresses alongside insignificant variances in cytosolic levels of  $\text{Ca}^{2+}$  or ATP,<sup>19</sup> is difficult to resolve, as the small non-metabolizable<sup>9</sup> and highly abundant<sup>13</sup> amino acid can have multiple targets of varying affinity within the cell.

In this study, we detail the long-term intracellular interaction partners of taurine signalling, using pharmacological insulinotropic tools, and dissect the structural basis of fast-scale amino acid handling by the taurine transporter. Utilizing a clonal  $\beta$ -cell screening system and insulin secretion as a read-out, we demonstrate the structural specificity for the transport of taurine homologs and strong synergism of taurine and membrane depolarization and GLP-1 signalling over an extended timescale.

## 2 | MATERIALS AND METHODS

### 2.1 | Reagents

All chemicals were obtained from Sigma-Aldrich (Poole, Dorset, UK) unless stated otherwise.

### 2.2 | Animals and islet isolation

All animal experiments were conducted under the United Kingdom Animals (Scientific Procedures) Act (1986) and

the Ulster University ethical guidelines. C57Bl/6J mice (12–18 weeks, Charles River, UK) and adult male Wistar rats (Harlan, UK) were maintained in a conventional vivarium with a 12-h dark/light cycle and free access to food and water. The animals were killed by cervical dislocation, and samples of tissues were retrieved for further analysis. Islets of Langerhans were isolated by injecting ice-cold collagenase solution into the bile duct, followed by digestion of the connective and exocrine pancreatic tissue.<sup>20</sup> For imaging studies, islets were cultured for 48 h in RPMI medium, supplemented with 10% FBS, 100 IU/mL penicillin, and 100  $\mu\text{g}/\text{mL}$  streptomycin (Life Technologies, Paisley, UK) in a fully humidified atmosphere with 5%  $\text{CO}_2$ , at  $+37^\circ\text{C}$ . Recombinant reporters of  $\text{Ca}^{2+}$  (GCaMP6f, Vector Biolabs, USA), Perceval (ATP/ADP),<sup>21</sup> and Hylight (fructose 1,6-bisphosphate, FBP)<sup>22</sup> were delivered adenovirally ( $10^5$  IU/islet), followed by a 24-h culture to express the protein.

Human pancreatic islets were isolated from non-diabetic donors in the Oxford Diabetes Research & Wellness Foundation Human Islet Isolation Facility, as detailed in Refs. [23,24].

### 2.3 | Imaging of cytosolic $[\text{Ca}^{2+}]$ , fructose 1,6-bisphosphate, ATP/ADP, and NAD(P)H

Fluorescence of recombinant sensors expressed by the peripheral layer of islet cells<sup>25</sup> was imaged on a Zeiss LSM510-META confocal microscope, using a  $20\times/0.75$  objective or Zeiss AxioZoom.v16 wide-field microscope equipped with a  $2.3\times/0.56$  objective. Fluorescence of GCaMP6f, Perceval, and Hylight, reporting cytosolic  $[\text{Ca}^{2+}]$ , ATP/ADP,<sup>21</sup> and fructose 1,6-bisphosphate,<sup>22</sup> respectively, was excited at 490 nm, and imaged at 530 nm. The NAD(P)H autofluorescence was excited at 370 nm and imaged at 450 nm. The images were acquired every 8 s (GCaMP6f) or 60 mins (the rest) at  $+37^\circ\text{C}$ , while the islets were perfused continuously with extracellular solution EC1, containing, in mM: 140 NaCl, 4.6 KCl, 2.6  $\text{CaCl}_2$ , 1.2  $\text{MgCl}_2$ , 1  $\text{NaH}_2\text{PO}_4$ , 5  $\text{NaHCO}_3$ , 10 HEPES (pH 7.4, with NaOH), 0.2% BSA, and agonists as indicated (Figure 1B).<sup>9</sup>

### 2.4 | Clonal $\beta$ - and $\delta$ -cells and immunocytochemistry

Clonal rat pancreatic BRIN-BD11 cells<sup>26</sup> were grown in RPMI 1640 medium (as above). Clonal  $\delta$ -cell line, TGP-52,<sup>27,28</sup> was maintained in DMEM/Ham's F12 (1:1) medium containing 17.5 mM glucose, supplemented with 10% FBS, 100 IU/mL penicillin, and 0.1 mg/mL streptomycin (Life Technologies, Paisley, UK). For immunocytochemistry, cells grown on

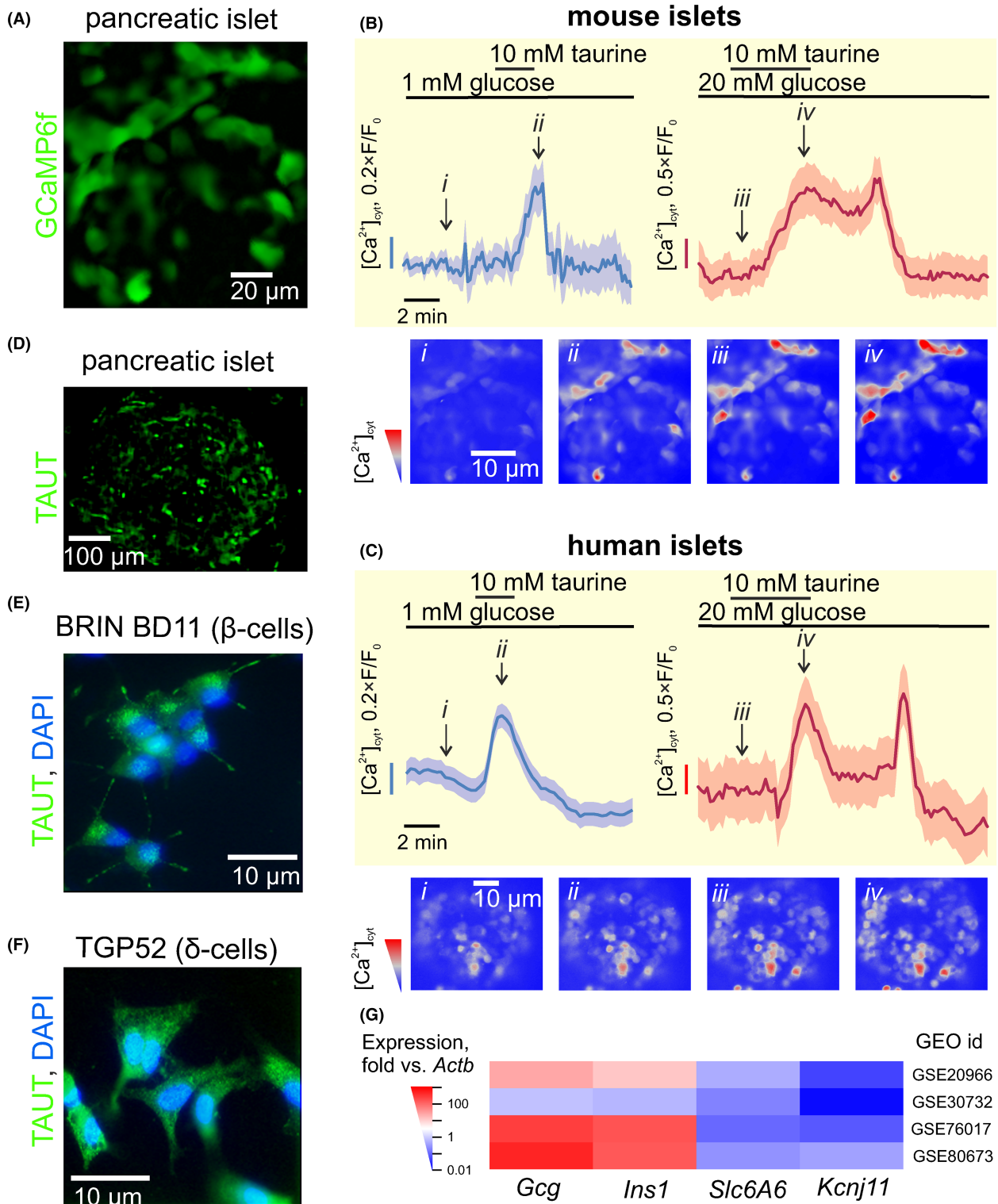


**FIGURE 1** Taurine transporter is expressed in primary and clonal pancreatic islet cells. (A) Confocal image of the pancreatic islet expressing GCaMP6f  $\text{Ca}^{2+}$  sensor. (B, C) *Top*: Dynamics of  $[\text{Ca}^{2+}]_{\text{cyt}}$  in mouse (B) and human (C) pancreatic islet  $\beta$ -cells in response to the application of taurine (10 mM), at low (1 mM) and high (20 mM) glucose ( $n=313$  cells from 5 mice;  $n=417$  cells from 3 donors). *Bottom*: color-coded images of GCaMP6f fluorescence in islet cells at the time points *i-iv*, as indicated in the plots above. (D–F) Immunofluorescence staining of rat pancreatic islet (C) BRIN-BD11  $\beta$ -cell (D) and TGP52  $\delta$ -cell (E) lines for the taurine transporter, TauT. (G) Expression of the taurine transporter mRNA, *Slc6A6*, alongside glucagon (*Gcg*), insulin (*Ins1*), and pore subunit of  $\text{K}_{\text{ATP}}$  channel (*Kcnj11*) in human (GSE20966 and GSE30732) and mouse (GSE76017 and GSE80673) pancreatic islets. The expression levels were normalized to that of *Actb*.



glass coverslips were fixed with 4% PFA (48 h, +4°C). The samples were blocked with 2% BSA and incubated with primary (overnight, +4°C) and secondary antibodies, as specified, followed by incubation with DAPI (300 nM, at +37°C) to stain the nuclei. The stained samples were imaged using an Olympus BX51 microscope, equipped with a 40×/1.3 objective. The fluorescence was recorded using DAPI (excitation 350 nm/emission 440 nm), FITC (488/515), and TRITC (594/610) filters and a DP70 camera controlled by Cell<sup>F</sup> software (Olympus, UK).

## 2.5 | qRT-PCR

BRIN-BD11 cells were seeded at  $2 \times 10^5$  cells/well in a six-well plate, allowed to attach for 6 h, and cultured for further 12 h. To probe the expression of TauT mRNA, cells (or tissues isolated from animals, as indicated) were washed with HBSS solution, lysed using Trizol, and centrifuged at 16 000g (10 min at +4°C). mRNA was extracted from the supernatant using chloroform-isopropanol and reverse transcribed using a Superscript II reverse transcriptase-RNase H kit (Invitrogen, UK, +42°C, 50 min). RT-PCR was performed using the forward (5'-ATTGTCATCCTCCTCTGCCG-3) and reverse (5'-TCTGGAGTGAAAGGCGGTAG-3) primers on a MiniOpticon two-color real-time PCR detection system (BioRad, UK). Data evaluation was performed using the  $\Delta\Delta C_t$  method, using *ACTB* ( $\beta$ -actin) as a housekeeping gene.

## 2.6 | Hormone secretion

Monolayers of BRIN-BD11 cells were established following seeding at a density of  $2 \times 10^5$  cells per well in 24-well (Falcon, New Jersey, U.S.A.) overnight, after which the culture medium was replaced by 1 mL of extracellular solution (EC2), containing, in mM: 115 NaCl, 4.7 KCl, 1.2 MgSO<sub>4</sub>, 1.28 CaCl<sub>2</sub>, 1.2 KH<sub>2</sub>PO<sub>4</sub>, 25 HEPES, 1 NaHCO<sub>3</sub>, 0.01% BSA, glucose as indicated, and pH 7.4 with NaOH. A 40-min pre-incubation at 1.1 mM glucose was followed by a 20 min incubation in 1 mL of the test solution, as indicated. The exposure time was chosen to reflect the effects on the first (Ca<sup>2+</sup>-driven) phase of insulin secretion.<sup>29</sup> Aliquots of the incubation buffer were subsequently removed and analyzed using insulin radioimmunoassay.<sup>30</sup>

## 2.7 | High-throughput imaging in cell lines

Dynamics of plasma membrane electrical potential and [Ca<sup>2+</sup>]<sub>cyt</sub> in the populations of BRIN-BD11 cells were

recorded using a FLIPR Membrane Potential Assay Kit and a FLIPR Calcium Assay Kit (Molecular Devices, Sunnyvale, CA, U.S.A.), respectively. BRIN-BD11 cells seeded in 96-well microplates (black walls, clear bottom, Costar, Roskilde, Denmark) at  $1 \times 10^5$  cells/well were pre-cultured for 18 h at +37°C to allow the attachment. The cells were subsequently pre-incubated in 100  $\mu$ L of EC2-containing 5.6 mM glucose and loaded with the respective FLIPR dye (100  $\mu$ L) in assay buffer for 60 min. The removal of extracellular Ca<sup>2+</sup> was modeled by omitting CaCl<sub>2</sub> from the EC2 solution and supplementing 0.5 mM EGTA instead. Na<sup>+</sup>-free solution, EC3, contained, in mM: 250 sucrose, 4.9 KCl, 1.28 CaCl<sub>2</sub>, 1.2 MgCl<sub>2</sub>, 1.2 KH<sub>2</sub>PO<sub>4</sub>, 25 HEPES, 1 KHCO<sub>3</sub>, and pH 7.4 with KOH. The signals were detected in a FlexStation 3 scanning fluorimeter utilizing a fluid transfer workstation (Molecular Devices, USA) for perfusion (78  $\mu$ L/s).<sup>31</sup> The dyes were excited at 485 nm, with the emission collected at 525 nm. The acquisition was performed for 10 min, at 0.4 Hz.

## 2.8 | Data analysis

Microscopic images were analyzed using FIJI (<http://fiji.sc/Fiji>). 3D rendering (Figure 3E) was performed using MolView (<https://molview.org>). The meta-analysis of the gene expression data deposited in GEO database was performed using Orange. Statistical analysis was performed using R<sup>32</sup> and IgorPro (Wavemetrics). Data are presented as the mean  $\pm$  SEM or heatmaps with the indicated significance of differences versus respective controls and numbers of experiments. The Mann–Whitney U-test (Wilcoxon signed-rank test) was used to determine the significance of the differences between independent (dependent) samples. Multiple comparisons within one experiment were performed using the Kruskal–Wallis test or the Friedman test with Nemenyi post-hoc analysis.

## 3 | RESULTS

### 3.1 | Taurine transporter TauT is abundant in pancreatic islet cells

Taurine (10 mM) acutely induced [Ca<sup>2+</sup>]<sub>cyt</sub> dynamics in mouse (Figure 1A,B) and human (Figure 1C) pancreatic islet cells, at both basal (1.1) and suprathreshold (16.7 mM) glucose concentrations. TauT (*Slc6a6*), the hypothetical conduit for taurine transport into the cytosol, was detectable immunocytochemically on the membrane of primary pancreatic rat islet cells (Figure 1D) and clonal  $\beta$ - (BRIN-BD11) and  $\delta$ -cells (TGP-52) (Figure 1E,F). *Slc6a6*

mRNA, abundant in human<sup>33,34</sup> and rodent<sup>35,36</sup> islets (Figure 1G), was also expressed in the BRIN-BD11 cells as well as in rat lung, heart, and, to a lesser extent, liver and kidney (Figure S1A). Probing the expression of TauT revealed the presence of two main translation products, 69 and 107 kDa,<sup>37</sup> that were not restricted to the membrane fraction, in rat liver and BRIN-BD11 cells (Figure S1A).

### 3.2 | Taurine homologs enhance insulin secretion in a glucose-dependent way

We mapped the architecture of the substrate-binding site of the taurine transporter by probing its function with a range of the structural homologs of taurine.<sup>8</sup> At low glucose, the acute addition of taurine, its close precursor, hypotaurine, and a rare analog, homotaurine, induced and dose dependently enhanced insulin release from BRIN-BD11 cells (Figure 2A–C,J). Significant potentiation of secretion was also recorded for small non-sulfur-containing amino acids GABA and  $\beta$ -alanine (Figure 2D,E,J), whereas larger sulfur-containing homologs produced very small (PIPES) or no (cysteic acid, cysteine sulfinic acid, and ACES) effect (Figure 2F–J).

Added at high (16.7 mM) glucose, taurine dose dependently potentiated insulin release, exhibiting a potent additive effect to that of the sugar, with an  $EC_{50}$  of around 2 mM (Figure 2A,K). Similarly, hypotaurine, homotaurine, GABA, and  $\beta$ -alanine produced dose-dependent additive potentiation with comparable pharmacodynamics (Figure 2B–E,K). The effect of PIPES and ACES, albeit significant, was much smaller (Figure 2F,I,K), whereas cysteic acid and cysteine sulfinic acid produced a dose-dependent inhibition of hormone secretion (Figure 2G,H,K).

### 3.3 | Insulin secretion induced by taurine homologs is not amplified by PKC activation

Having previously established that taurine import depolarizes the  $\beta$ -cell plasma membrane in an NKCC-dependent manner,<sup>8</sup> we explored signalling interactions for taurine and its homologs in the cell. Added acutely at 16.7 mM glucose, taurine,  $\beta$ -alanine, hypotaurine, GABA, and homotaurine (all at 10 mM, Figure 3D) significantly enhanced insulin secretion in BRIN-BD11 cells (Figures 2A–E and 3B). The acute effect was associated with membrane depolarization (Figure 3C) and elevation of  $[Ca^{2+}]_{\text{cyt}}$  (Figure 3C), in line with the  $[Ca^{2+}]_{\text{cyt}}$  imaging data (Figure 1B).

Added upon the plasma membrane depolarization with 30 mM KCl (Figure 3A), taurine produced a small but significant ( $1.3 \pm 0.3$ -fold) enhancement of insulin release, a feat accomplished, to a lesser extent, by  $\beta$ -alanine but not

hypotaurine (Figure 3B). Notably, GABA and homotaurine, in turn, attenuated insulin secretion induced by 30 mM KCl (Figure 3B). Taurine exhibited the profile of strong “all-rounder” additive secretagogue, being able to enhance insulin secretion induced via various mechanisms linked to plasma membrane depolarization (tolbutamide,  $2.3 \pm 0.4$ -fold),  $Ca^{2+}$  influx (high extracellular  $Ca^{2+}$ ,  $3.2 \pm 0.3$ -fold), activation of PKC (PMA,  $2.6 \pm 0.3$ -fold), or elevation of intracellular cAMP levels (forskolin,  $2.6 \pm 0.4$ -fold; GLP-1,  $3.0 \pm 0.2$ -fold) (Figure 3B). This profile was closely replicated by  $\beta$ -alanine, hypotaurine, and, to a lesser extent, homotaurine, with the marked exclusion of the interaction with PKC signalling (Figure 3B). At the same time, GABA produced a much smaller additive effect that was barely detectable on the background of forskolin or PMA (Figure 3B).

Notably, assayed at the level of  $[Ca^{2+}]_{\text{cyt}}$  dynamics in primary mouse islet cells, the effects of taurine, hypotaurine, homotaurine, and GABA were significantly attenuated by administration of competitive antagonist of TauT, piperidine-4-sulfonate<sup>38</sup> (10 mM) (Figure 3E).  $\beta$ -Alanine was still able to invoke a response, albeit at a significantly lower scale (Figure 3E).

### 3.4 | Pre-culturing in taurine dose dependently augments the effects of GLP-1 and the elevation of $[Ca^{2+}]_{\text{cyt}}$ on glucose-induced insulin secretion

In our hands, taurine had a bimodal impact on islet  $\beta$ -cell metabolism and signalling, depending on the duration of the exposure to the amino acid.<sup>9</sup> We, therefore, complemented the acute observations (Figure 3) by profiling the interaction partners for chronically administered taurine. To that end, 11 secretagogues were screened for functional interaction with 18-h culture in 2 or 20 mM of taurine (Figure 4). Culturing in the presence of taurine had no impact on insulin content and cell viability (Figure 1C). At 16.7 mM glucose, there were potent additive insulinotropic effects between chronic taurine and acutely administered GLP-1 ( $1.2 \pm 0.1$ -fold vs. 0 mM taurine culture,  $p < 0.01$ ), membrane depolarization with 30 mM KCl ( $1.1 \pm 0.1$ -fold,  $p < 0.05$ ), tolbutamide ( $1.3 \pm 0.3$ -fold,  $p < 0.05$ ), elevated extracellular  $Ca^{2+}$  ( $1.3 \pm 0.3$ -fold,  $p < 0.01$ ), or release of the luminal  $Ca^{2+}$  by carbachol ( $1.1 \pm 0.1$ -fold,  $p < 0.01$ ) (Figure 4B). Importantly, the effect of the acute addition of GLP-1 to 16.7 mM glucose, as well as that of carbachol, KCl, and high extracellular  $Ca^{2+}$  (Figure 4A), was dose-dependently upregulated by taurine in the culture medium (Figure 4B).

At the same time, forskolin (25  $\mu$ M) weakly potentiated the effect of glucose only in 2 mM taurine culture, whereas, in 20 mM taurine culture, the labdane inhibited glucose-induced insulin secretion by 10% (Figure 4B). Likewise,

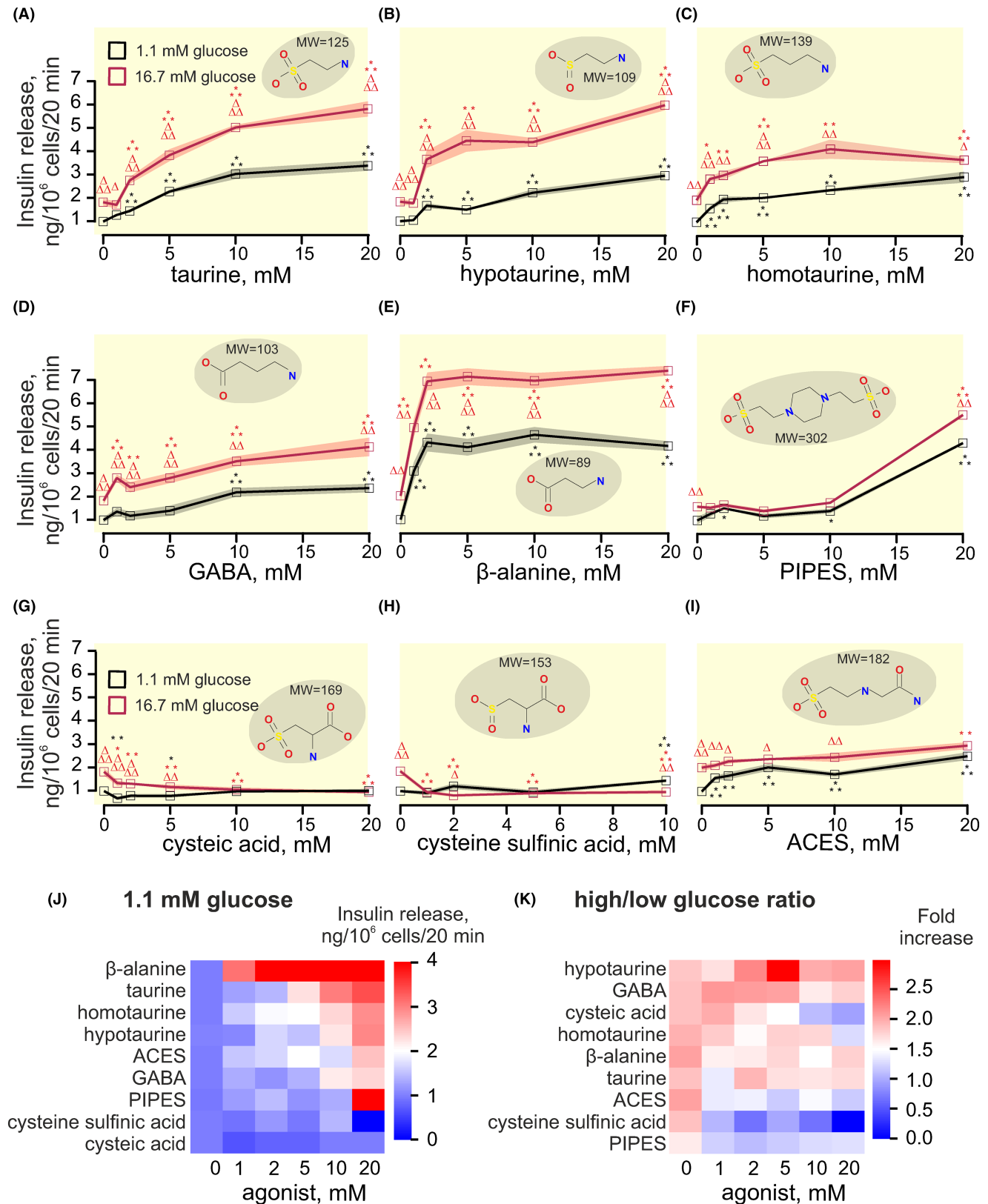


**FIGURE 2** Taurine homologs enhance insulin secretion via a glucose-dependent mechanism. (A–I) Dose–response of the acute (20 min) stimulation of insulin secretion by taurine (A), hypotaurine (B), homotaurine (C), GABA (D), β-alanine (E), PIPES (F), cysteic acid (G), cysteine sulfinic acid (H), or ACES (I), at basal (1.1 mM, black) or stimulatory (16.7 mM, red) glucose concentrations in BRIN BD11 β-cells ( $n=6$ ). \*\* $p < 0.01$ , \*\*\* $p < 0.001$  compared with respective effect in the absence of the agent.  $\Delta p < 0.05$ ,  $\Delta\Delta p < 0.001$  compared with respective effect at low glucose. (J, K) Comparison of basal (1.1 mM glucose) secretion induced by the agonists above (J) and the impact of high (16.7 mM) glucose on secretion induced by the amino acids (K). The data, derived from A–I, is ranked by the size of the stimulatory effect at 1 mM glucose (J) or the degree of glucose dependence of the potentiation (K).

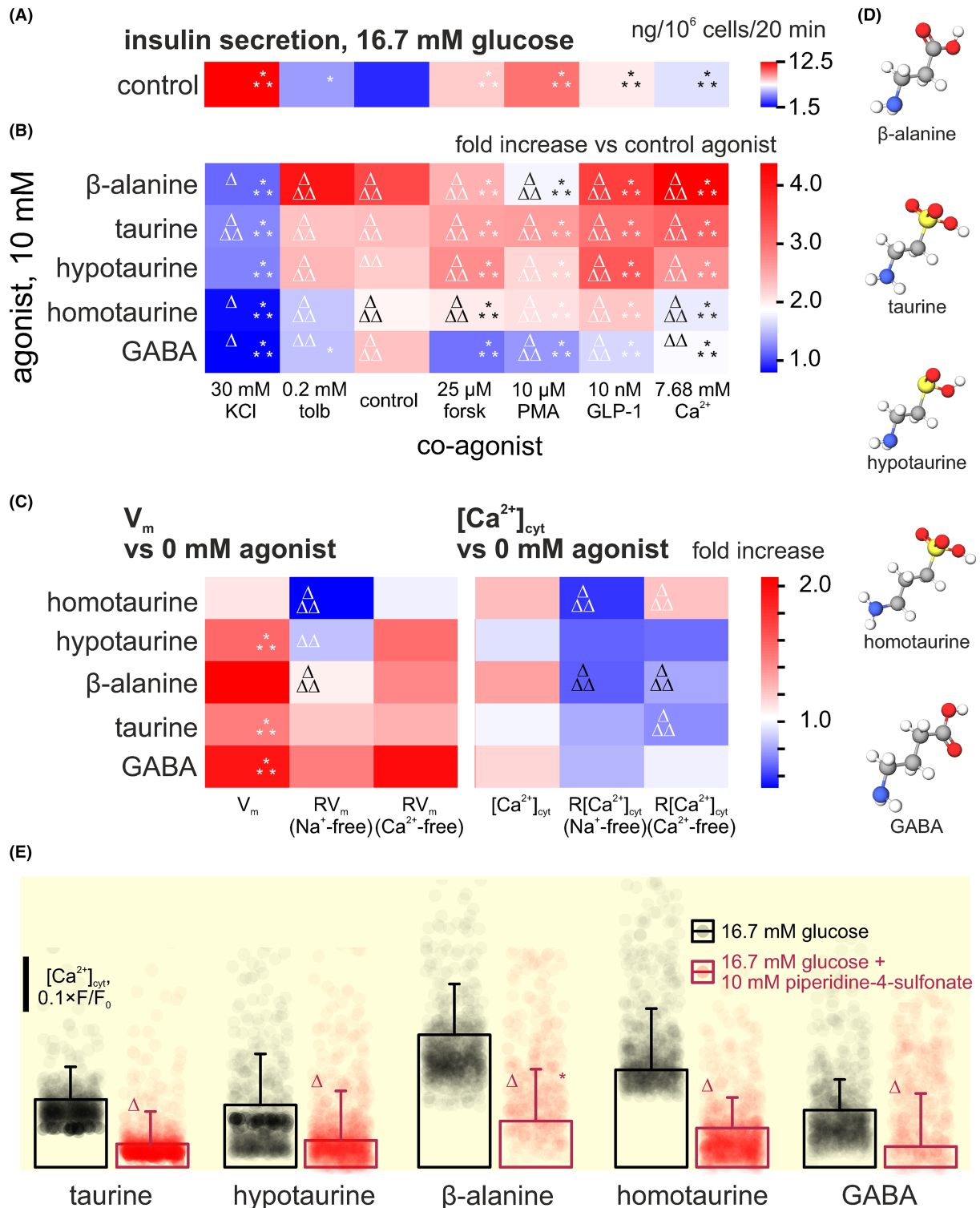


FIGURE 3 Legend on next page

other compounds tested produced dose-dependent (proline, taurine, and alanine) or -independent (PMA and cholecystinin) inhibition of glucose-induced insulin secretion (Figure 4B).

In line with the findings in the clonal system, pre-culture in taurine significantly enhanced glucose-induced Ca<sup>2+</sup> influx (Figure 4C,D) and attenuated the responses of

intracellular cAMP (Figure 4E,F) and DAG (Figure 4G,H) to the respective agonists in primary mouse and human islet cells. Furthermore, 18-h culture in taurine enhanced glycolytic flux in mouse islets (Figure 5A,B), but had only a small effect on the production of ATP that was inhibited by hyperpolarizing the plasma membrane with K<sub>ATP</sub> channel opener diazoxide (Figure 5D,E).



### 3.5 | GLP-1 sensitizes $\beta$ -cells to the acute taurine stimulus

The additive effect of taurine and GLP-1 (Figures 3 and 4) was further dissected to probe the dose dependence of acute and chronic interaction between the two signalling pathways. Added acutely (20 min), taurine dose dependently induced insulin secretion from BRIN-BD11 cells at low glucose (1.1 mM) (Figure 6A), which was enhanced by high glucose (16.7 mM), with a marked synergism between the two secretagogues peaking at 2 mM taurine (Figure 6A). The addition of 10 nM GLP-1 further potentiated insulin release induced by glucose and taurine (Figure 6B). The added effect of GLP-1 on insulin secretion, however, shifted the peak of taurine efficacy to 1 mM thereby sensitizing the cell to the amino acid (Figure 6B).

Eighteen hours pre-culture in 10 mM taurine resulted in a significant potentiation of acute effects of membrane depolarization with 30 mM KCl, high extracellular  $\text{Ca}^{2+}$ , GLP-1, and tolbutamide ( $p < 0.001$  and  $p < 0.01$  vs. taurine-free culture) (Figure 6C). At the same time, 18-h pre-culturing in 10 nM GLP-1 significantly attenuated the secretory response to every acute agonist (Figure 6C), whereas the combination of GLP-1 and taurine in the culture had no significant impact on the secretory responses (Figure 6C).

### 3.6 | Taurine rescues insulinostatic effects of chronic exposure to $\text{K}_{\text{ATP}}$ channel inhibitors

Similar to GLP-1, the membrane depolarizing agents displayed strong additivity to both acute and chronic supplementation of taurine (Figures 3 and 4). We, therefore, explored the dose dependence of acute and chronic interaction between taurine and  $\text{K}_{\text{ATP}}$  channel inhibitors, sulfonylurea tolbutamide and meglitinide nateglinide.

Assayed at 16.7 mM glucose, tolbutamide and nateglinide (both at 100  $\mu\text{M}$ ) had a significant impact on the potentiation of insulin secretion by taurine in BRIN-BD11 cells (Figure 7A,B), an effect decreasing with increasing taurine concentration (Figure 7A,B). Pre-culturing with either of the  $\text{K}_{\text{ATP}}$  channel inhibitors reduced the response to the acute addition of the secretagogues (Figure 7C), with the addition of taurine in the culture partially rescuing this tendency (Figure 7C).

## 4 | DISCUSSION

While several mechanisms have been implicated in the intracellular transport of neutral amino acids,<sup>39,40</sup> there is little debate about the essential role of TauT, a  $\text{Na}^+/\text{Cl}^-$ -dependent transporter, in taurine import into pancreatic islet  $\beta$ -cells.<sup>8,41</sup> The experimental approach was chosen to allow a reliable comparison of the effect of multiple taurine analogs, exploiting the lack of acute metabolic effects of the amino acid in islets in  $\beta$ -cells.<sup>8,9</sup> Using a set of homologous molecular probes,<sup>42</sup> the present study demonstrates that taurine transport into the  $\beta$ -cell is sensitive to the spatial geometry of the amino acid rather than the presence of the SH- group (Figure 2). Administered acutely, taurine dose dependently potentiated the insulinotropic effects of all the “mainstream” secretagogues save KCl (Figure 3). On the chronic timescale, taurine synergistically interacted with GLP-1/cAMP signalling, abrupt depolarization of plasma membrane, and potentiation of  $\text{Ca}^{2+}$  influx (Figures 6 and 7) but not the amino acids and PKC agonists (Figure 4).

### 4.1 | Ligand specificity of TauT

Taurine transporter TauT (*Slc6a6*) exhibited a broad expression pattern (Figures 1G and S1A), in line with earlier

**FIGURE 3** Co-stimulation of insulin secretion induced by taurine homologs. (A, B) Effects of the acute (20 min) co-stimulation of insulin secretion by taurine, hypotaurine, homotaurine, GABA, and  $\beta$ -alanine with agents depolarizing the plasma membrane (30 mM KCl and 0.2 mM tolbutamide), elevating the activity of PKA and EPAC2 (10 nM GLP-1 and 25  $\mu\text{M}$  forskolin) or PKC (10  $\mu\text{M}$  PMA) or direct elevation of extracellular  $\text{Ca}^{2+}$  to 7.68 mM, at stimulatory glucose concentration (16.7 mM) ( $n = 6$ ). “PMA,” Phorbol 12-myristate 13-acetate; “forsk,” forskolin; and “tolb,” tolbutamide. The data are ranked by the size of the overall stimulatory effect of the amino acid across the co-agonists. (C) Effects of the acute (20 min) application of taurine, hypotaurine, homotaurine, GABA, and  $\beta$ -alanine on the plasma membrane potential ( $V_m$ ) and cytosolic  $[\text{Ca}^{2+}]_{\text{cyt}}$  in BRIN-BD11 cells, at stimulatory glucose concentration (16.7 mM). Effects are reported in the presence ( $V_m$ ,  $[\text{Ca}^{2+}]_{\text{cyt}}$ ) or without extracellular  $\text{Na}^+$  ( $\text{RV}_m$  ( $\text{Na}^+$ -free),  $\text{R}[\text{Ca}^{2+}]_{\text{cyt}}$  ( $\text{Na}^+$ -free)) or  $\text{Ca}^{2+}$  ( $\text{RV}_m$  ( $\text{Ca}^{2+}$ -free),  $\text{R}[\text{Ca}^{2+}]_{\text{cyt}}$  ( $\text{Ca}^{2+}$ -free)) ( $n = 6$ ). The data are ranked by the impact of the amino acid on  $V_m$ . \* $p < 0.05$ , \*\*\* $p < 0.001$  compared with respective effect in the absence of the respective secretagogue (A) or in the presence of  $\text{Na}^+$  or  $\text{Ca}^{2+}$  (B), that is, versus the control condition.  $\Delta p < 0.05$ ,  $\Delta\Delta p < 0.01$ ,  $\Delta\Delta\Delta p < 0.001$  compared with respective effects in the absence of the taurine homolog. (D) 3D-rendered molecular structures of the taurine homologs indicating atoms: N (blue), S (yellow), O (red), C (gray), and H (white). (E) Effect of the inhibition of TauT activity (with 10 mM of piperidine-4-sulfonate) on  $[\text{Ca}^{2+}]_{\text{cyt}}$  dynamics induced by taurine homologs in primary mouse islets ( $n = 895$  cells from three preparations).  $\Delta^{(*)}p < 0.05$ , compared with the solution lacking the antagonist (glucose).



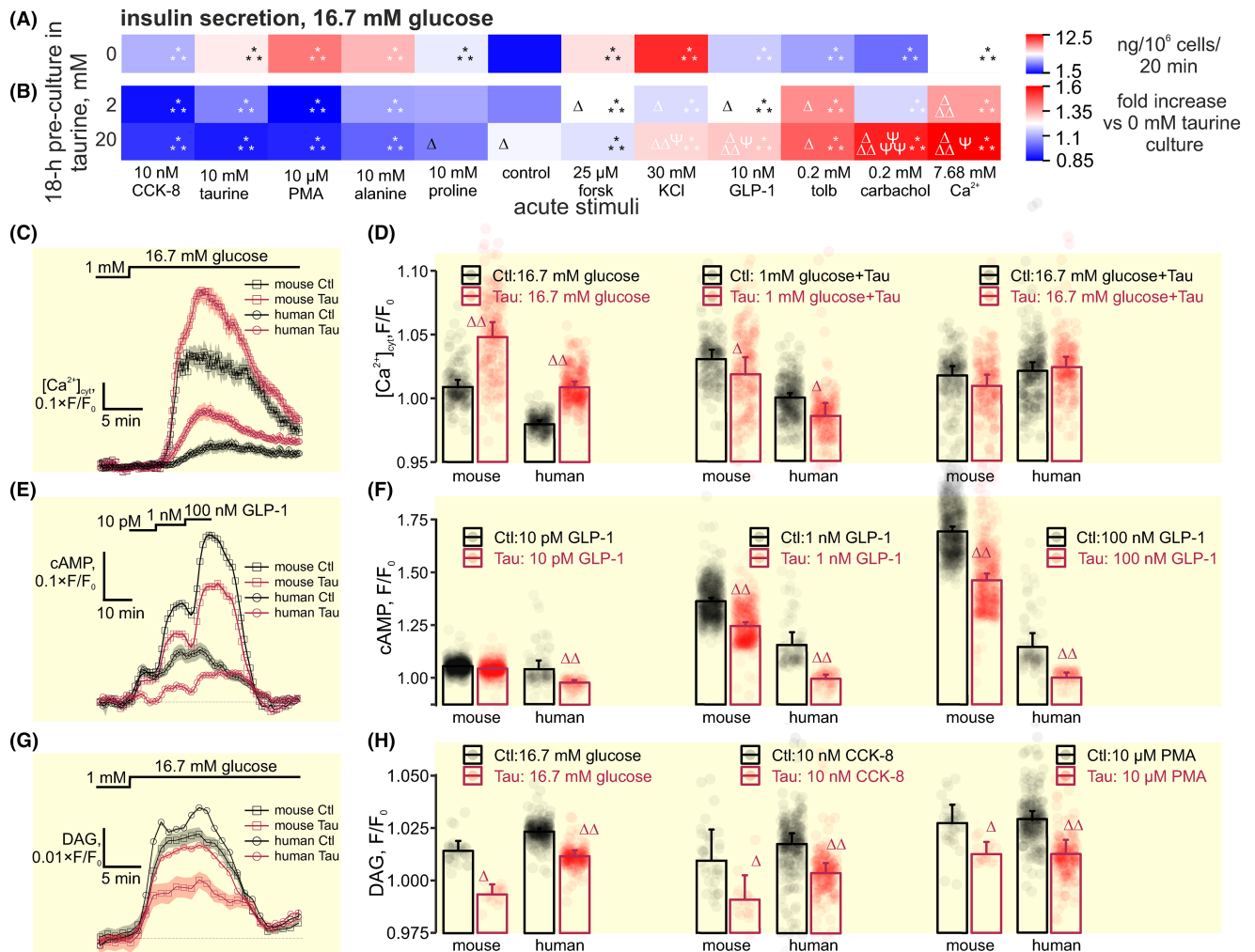


**FIGURE 4** Pre-culturing in taurine dose dependently augments the effects of GLP-1 and the elevation of  $[Ca^{2+}]_{cyt}$  on glucose-induced insulin secretion. Effects of 18 h pre-culturing of BRIN-BD11  $\beta$ -cell line with taurine (0, 2, and 20 mM) on acute insulinotropic actions of various secretagogues, as indicated, at 16.7 mM glucose ( $n=6$ ). The data are ranked by the strength of the potentiation of the secretion induced by pre-culturing in taurine. “CCK8,” cholecystikinin; “PMA,” Phorbol 12-myristate 13-acetate; “forsk,” forskolin; “tolb,” tolbutamide. (A) Insulin secretion ( $ng/10^6$  cells/20 min) in response to the acute exposure of secretagogues indicated in the absence of taurine. (B) Fold increase of the secretory output (as in the top panel) by pre-culturing in 2 or 20 mM taurine, as indicated. (C–H) Effects of 18-h culture in 20 mM taurine on intracellular signalling in mouse and human islets of Langerhans, assayed at the level of  $[Ca^{2+}]_{cyt}$  response to high glucose (C, D) ( $n=166$  (180) and  $n=274$  (197) cells from three preparations for mouse and human control (taurine) groups), cAMP response to 10 pM, 1 nM, and 100 nM GLP-1 (E, F) ( $n=689$  (506) and  $n=897$  (546) cells from three preparations for mouse and human control (taurine) groups), and DAG response to high glucose, CCK-8, and PMA (G, H) ( $n=72$  (51) and  $n=257$  (199) cells from three preparations for mouse and human control (taurine) groups). \*\*\* $p < 0.001$  versus control (absence of the agent).  $\Delta p < 0.05$ ,  $\Delta\Delta p < 0.01$ ,  $\Delta\Delta\Delta p < 0.001$  versus respective condition in the absence of taurine pre-culture.  $\Psi p < 0.05$ ,  $\Psi\Psi\Psi p < 0.001$  versus respective condition at 2 mM taurine pre-culturing.

research advocating the osmolyte role for taurine.<sup>43</sup> The expression of TauT in islet cells and  $\beta$ - and  $\delta$ -cell lines echoes wide-scale studies<sup>44–46</sup> and complements our earlier findings of the anti-apoptotic/proliferative effect of taurine in  $\beta$ -cells.<sup>9</sup>

Using insulin secretion as a surrogate reporter, we recorded a significant influx of non-sulfur-containing  $\beta$ -amino acids but not large amino-sulfonic acids into the

$\beta$ -cell (Figure 2). Although the transport of the assayed amino acids can be accomplished via other routes, the observation above reveals the TauT topology: the sulfur-containing group proved to be less critical for the recognition of the amino acid by the transporter than the ligand size.

Earlier studies using site-directed mutagenesis suggested taurine uptake by TauT to be defined by three polar residues

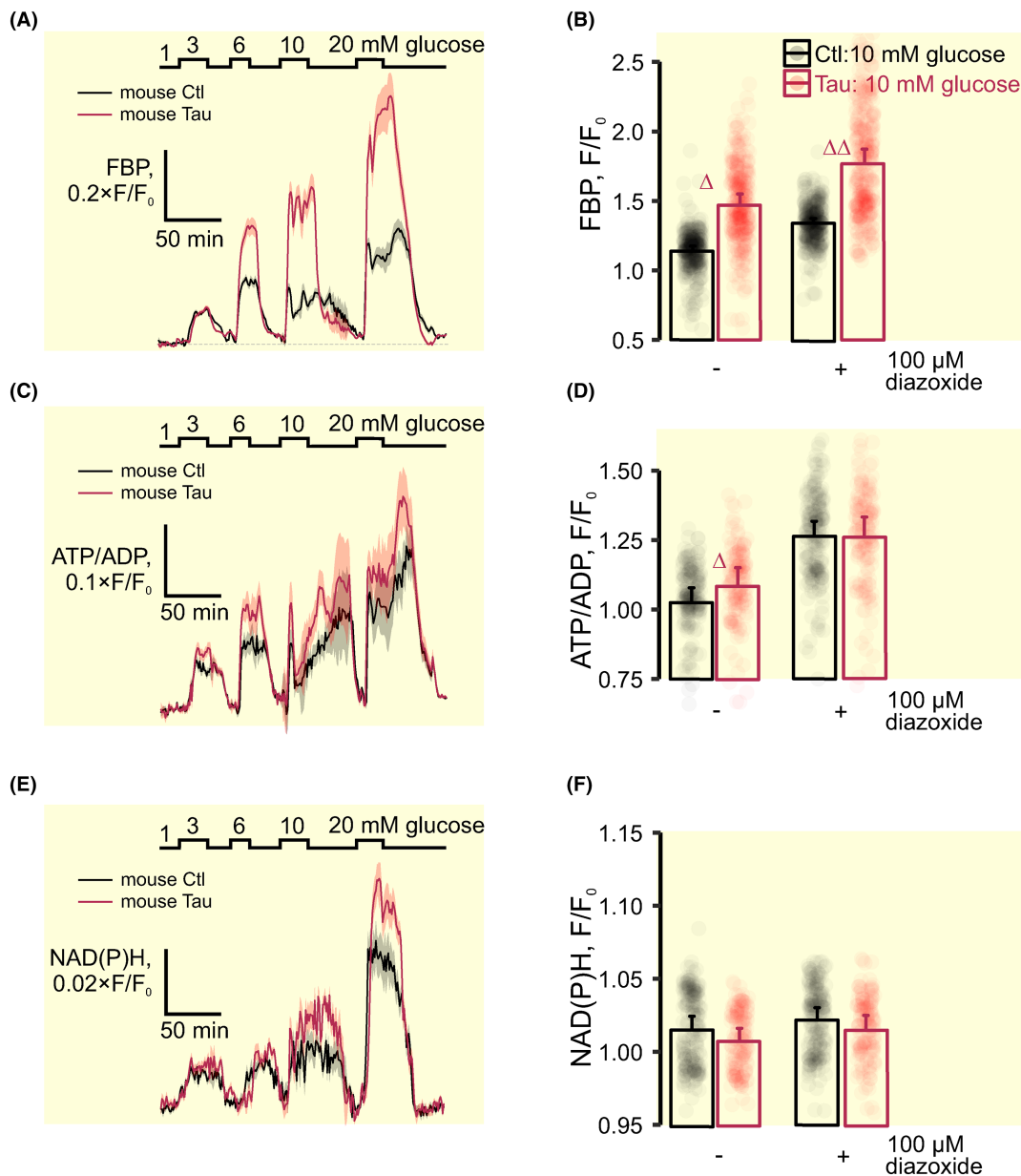
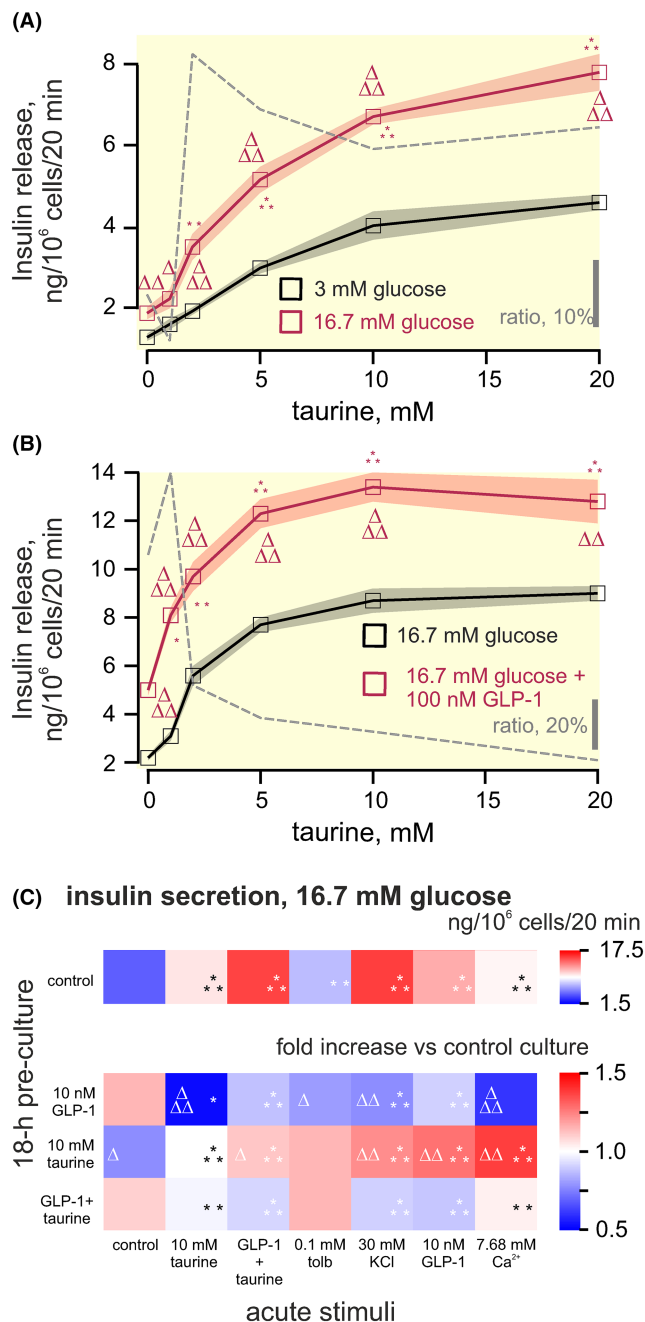


**FIGURE 5** Metabolic impact of taurine culture. Effects of 18-h culture in 20mM taurine on energy metabolism in mouse islets of Langerhans, assayed at the level of FBP (A, B,  $n = 658$  from three preparations), ATP/ADP ratio (C, D,  $n = 427$ ), and NAD(P)H (E, F,  $n = 366$ ) response to high glucose.  $^{\Delta}p < 0.05$ ,  $^{\Delta\Delta}p < 0.01$  versus respective condition in the absence of taurine pre-culture.

within the intracellular segment S4 (K319, R324, and D325).<sup>47</sup> The proximity of the putative phosphorylation site for PKC,<sup>48</sup> however, suggests an allosteric modality of this regulation. A 1.6 nm crystal structure of a distant (19%) homolog, TauA, revealed an extracellular binding site for alkanesulfonates, assembled by Q30, G61, G79, E106, T132, and D205 residues.<sup>49</sup> Despite being located proximally to the conserved motifs (Figure 8A), none of the six residues is conserved in the mammalian homologs, with only D205, coordinating the binding of the ethylamine group, and corresponding to a similarly acidic E197 in TauT (Figure 8A). The weak coordination of sulfonate binding by TauT may explain the lack of selectivity to sulfonate-containing amino acids (Figure 2).

#### 4.2 | The acute taurine effect is potentiated by enhanced Ca<sup>2+</sup> entry and elevated cytosolic cAMP, but not by membrane depolarization or activation of PKC

As demonstrated earlier, taurine and other small neutral amino acids trigger [Ca<sup>2+</sup>]<sub>cyt</sub> dynamics in pancreatic islet cells,<sup>8,9</sup> a bona fide signal for the hormone exocytosis.<sup>50,51</sup> The effect relied on the membrane depolarization and Ca<sup>2+</sup> influx, as demonstrated via the omission of Na<sup>+</sup> and Ca<sup>2+</sup> from the extracellular solution (Figure 3B). Taurine or its homologs dramatically enhanced the hormone



release, added acutely under the depolarization of plasma membrane by 16.7 mM glucose (Figure 2) but not 30 mM KCl (Figure 3A), in line with the sharp dependence between the  $\beta$ -cell membrane  $K^+$  conductance and electrical potential.<sup>52</sup> Supplementing extra  $Ca^{2+}$  expectedly enhanced the triggering stimulus, whereas elevating cytosolic cAMP by GLP-1 potentiated the granule fusion during exocytosis (Figures 3B and 8B). The relatively smaller effect of forskolin may reflect the adverse metabolic impact of labdane,<sup>53</sup> which is likely to have a critical role in the late stages of granule fusion.<sup>54</sup> The surprising lack of insulin exocytosis potentiation by the activation of PKC (Figure 3B), a recognized modulator of TauT,<sup>48</sup> recorded for the homologs tested acutely (Figure 3B) and

**FIGURE 6** The effect of interaction between taurine and GLP-1 depends on the duration of exposure to taurine. (A, B) Mean taurine dose–response relationship for insulin secretion, recorded upon the acute (20 min) exposure to taurine in the presence of low (3 mM) or high (16.7 mM) glucose (A) or high glucose and GLP-1 (B). The dashed curve represents the ratio of potentiation by taurine at the stimulatory versus control (red curve vs. black curve) conditions. \* $p < 0.05$ , \*\* $p < 0.01$ , \*\*\* $p < 0.001$  compared with respective effect in the absence of the taurine.  $\Delta p < 0.05$ ,  $\Delta\Delta p < 0.01$ ,  $\Delta\Delta\Delta p < 0.001$  compared with respective effects at low glucose (A) or in the absence of GLP-1 (B). (C) Interaction between the effects of chronic 18-h pre-culture in the presence of 10 mM taurine, 100 nM GLP-1, or taurine with GLP-1 on insulin secretion, induced by the acute treatment with GLP-1, taurine, 30 mM KCl, and 100  $\mu$ M tolbutamide of high (7.68 mM) extracellular  $Ca^{2+}$ , at a stimulatory glucose concentration (16.7 mM). *Top*: absolute values of secretion induced by the acute stimuli in the control (taurine- and GLP-1-free) culture. *Bottom*: fold increase in insulin secretion versus the control culture. The data are ranked by the strength of the potentiation of the secretion induced by pre-culturing in taurine. “tolb,” tolbutamide. \* $p < 0.05$ , \*\* $p < 0.01$ , \*\*\* $p < 0.001$  compared with respective effect in the absence of the acute agent.  $\Delta p < 0.05$ ,  $\Delta\Delta p < 0.01$ ,  $\Delta\Delta\Delta p < 0.001$  compared with respective effect in the absence of the chronic agent (control culture).

in chronic taurine cultures (Figure 4), suggests that these compounds, at least in part, could be implementing their insulinotropic effects via the PKC pathway. At the same time, the reports on the effect of GABA on  $\beta$ -cell are controversial,<sup>55</sup> likely reflecting differences in intracellular  $Cl^-$  concentrations achieved in different labs.

### 4.3 | Long-term interactions of taurine in the $\beta$ -cell

Although systemic levels of predominantly exogenous<sup>56</sup> taurine range from 50  $\mu$ M<sup>57</sup> to 690  $\mu$ M,<sup>58</sup> depending on the dietary taurine supplementation, the cytosolic compartment, was reported to contain as much as 10-fold higher level of the amino acid than the plasma.<sup>56</sup> While acute addition of taurine depolarizes the plasma membrane of the  $\beta$ -cell, chronic exposure to elevated taurine levels reportedly remodeled  $\beta$ -cell energy metabolism, by attenuating mitochondrial oxidation in favor of anaplerosis (Figure 8B).<sup>8</sup> The interactomic profile for the chronic taurine effect reflected stronger synergism with the membrane depolarizing agents (KCl, tolbutamide) versus the acute effect of the amino acid (Figure 4); chronic taurine has, arguably, little effect on plasma membrane potential, in line with earlier reports.<sup>8</sup> The elevation of  $[Ca^{2+}]_{cyt}$  and cytosolic cAMP was strongly synergistic with chronic taurine, suggesting the latter has a small effect at the late  $Ca^{2+}$ /cAMP-dependent (but not PKC-dependent) stages of exocytosis. Thus, on the chronic timescale, taurine is

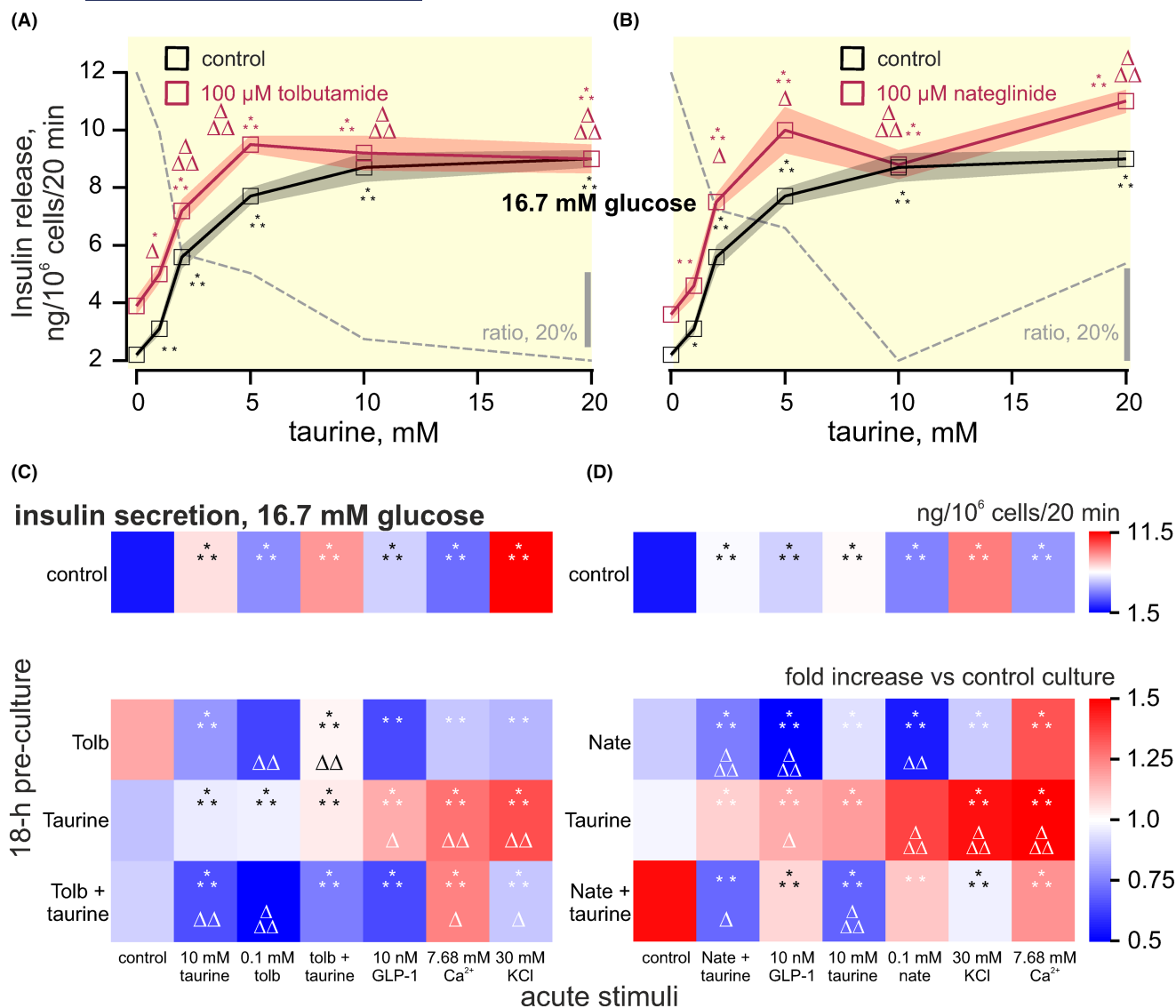


**FIGURE 7** The chronic potentiation of insulin secretion by taurine is additive to Ca<sup>2+</sup> and cAMP-dependent insulinotropic mechanisms. (A, B) Mean taurine dose–response relationship for insulin secretion, recorded upon the acute 20 min in the presence of high (16.7 mM) glucose and 100 μM of sulfonylurea tolbutamide (A) or meglitinide nateglinide (B). The dashed curve represents the ratio of potentiation by taurine at the stimulatory versus control (red curve vs. black curve) conditions. \**p* < 0.05, \*\**p* < 0.01, \*\*\**p* < 0.001 compared with respective effects in the absence of the taurine. Δ*p* < 0.05, ΔΔ*p* < 0.01, ΔΔΔ*p* < 0.001 compared with respective effects in the absence of tolbutamide (A) or nateglinide (B). (C, D) Interaction between the effects of chronic of 18 h pre-culture in the presence of 10 mM taurine, 100 μM tolbutamide, taurine with tolbutamide, or 100 μM nateglinide and taurine with nateglinide on insulin secretion (*n* = 6). The latter was induced by the acute treatment with GLP-1, taurine, 30 mM KCl, high (7.68 mM) extracellular Ca<sup>2+</sup>, 100 μM tolbutamide (C), or 100 μM nateglinide (D), alone or in combination with taurine, at a stimulatory glucose concentration (16.7 mM). *Top*: absolute values of insulin secretion induced by the acute stimuli in the control (taurine-, tolbutamide- (C). or nateglinide-free) culture. *Bottom*: fold increase in insulin secretion versus the control culture. The data are ranked by the strength of the potentiation of the secretion induced by pre-culturing in taurine. “nate,” nateglinide; “tolb,” tolbutamide. \*\**p* < 0.01, \*\*\**p* < 0.001 compared with respective effects in the absence of the acute agent. Δ*p* < 0.05, ΔΔ*p* < 0.01, ΔΔΔ*p* < 0.001 compared with respective effects in the absence of the chronic agent (control culture).

highly likely to affect PKC activity, not vice versa. The lack of potentiation of the amino acid-induced secretion in the taurine cultures likely stems from the saturation of the transport/signalling pathways.

A somewhat surprising observation was the opposite interaction profile of carbachol and CCK-8 (Figure 4), as the

targets of the two agents, subtypes of CCK-8<sup>59</sup> and muscarinic M3<sup>60</sup> receptors, are believed to be coupled to G<sub>q</sub> proteins, thereby sharing the machinery of the insulinotropic signalling. Recent reports of alternative, G<sub>s</sub> coupling for CCK-8 A receptor,<sup>61</sup> however, suggest that CCK8 effects could be in part mediated by changes in intracellular cAMP.



(B)

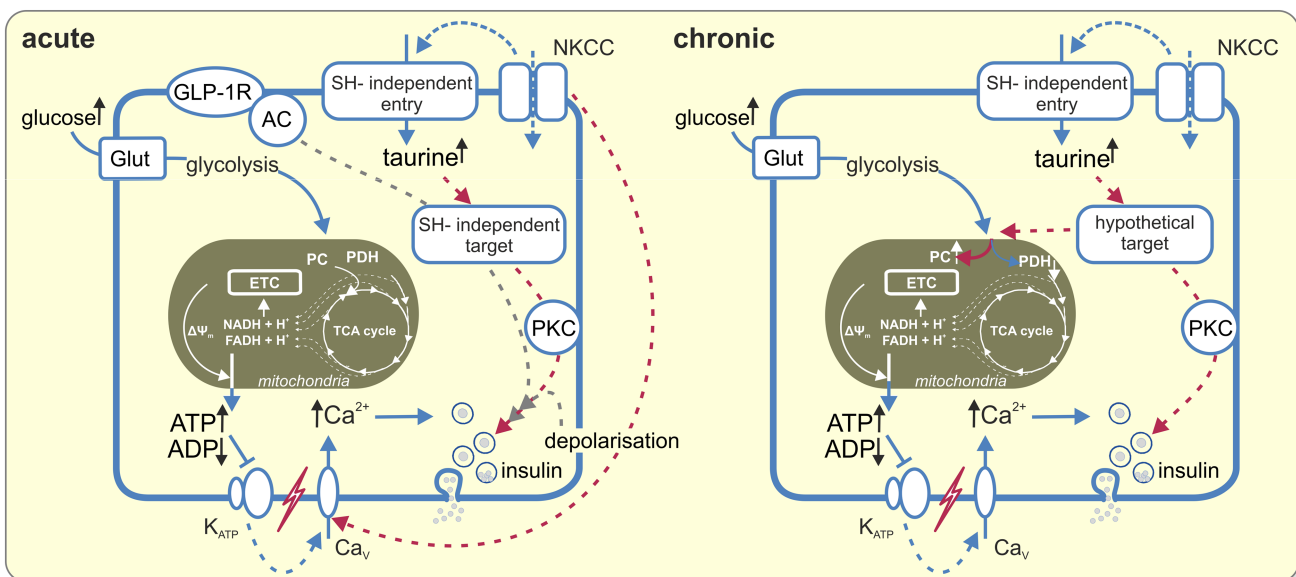


**FIGURE 8** Potential substrate-binding sites and mechanism of action in  $\beta$ -cell. (A) Clustal omega alignment of the amino acid sequence of *E. coli* TauA,<sup>49</sup> rat TauT, and canine TauT (derived from MDCK line)<sup>68</sup> transporters. The dashed squares indicate residues reportedly involved in substrate binding.<sup>14,49</sup> (B) Schematic of the proposed mechanism for acute and chronic taurine signalling in pancreatic  $\beta$ -cell. AC, adenylyl kinase; PKC, protein kinase C; ETC, electron transport chain; NKCC,  $Na^+K^+Cl^-$  co-transporter.

#### 4.4 | Interaction of taurine with antidiabetic drugs on the chronic timescale

The interaction between acute taurine and GLP-1 (Figure 6B) and  $K_{ATP}$  channel inhibitors (Figure 7A,B) predominantly decreased with increasing the concentration of the amino acid, whereas, under the chronic conditions, the overall effects were dominated by the refractory state

imposed in BRIN-BD11 cells by GLP-1 and  $K_{ATP}$  channel inhibitors (Figures 6C and 7C).

Whereas the mild interaction with  $K_{ATP}$  channel inhibitors (Figure 7A,B) reflects the acute depolarizing effect of taurine, the enhancement of the sensitivity to acute taurine by GLP-1 likely reflects a synergism between  $Ca^{2+}$  and cAMP dynamics in the  $\beta$ -cell.<sup>62</sup> On the chronic scale, the potentiation of glucose-induced insulin



secretion (Figure 8C, “control”) could be linked to the antiapoptotic effect of GLP-1,<sup>63</sup> whereas the attenuation of the acute stimulation by membrane depolarization or Ca<sup>2+</sup> (Figure 8C) may reflect metabolic rewiring induced by the incretin. Prolonged K<sub>ATP</sub> channel inhibition was reported to attenuate insulin granule dynamics,<sup>64</sup> alter gene expression,<sup>65</sup> and enhance the apoptosis<sup>66</sup> in  $\beta$ -cells, which, presumably, was partially combated by taurine (Figure 7C).

## 5 | CONCLUSION

With their acute insulinotropic effects mediated via membrane depolarization of the  $\beta$ -cell, the long-term roles of many amino acids depend on their specific intracellular targets that remain to be established. Similarly, the signaling downstream of the diet-derived taurine, mediating its impact on energy metabolism and selective interaction with acute GLP-1 (but not PKC) agonism,<sup>67</sup> prompts further in-depth studies.

### AUTHOR CONTRIBUTIONS

**Andrei I. Tarasov:** Conceptualization; investigation; writing – review and editing; methodology; validation; software; formal analysis; project administration. **Julie Turbitt:** Conceptualization; methodology; investigation; writing – original draft. **R. Charlotte Moffett:** Conceptualization; supervision; project administration; writing – review and editing. **Lorraine Brennan:** Conceptualization; writing – review and editing. **Paul R. V. Johnson:** Resources. **Peter R. Flatt:** Conceptualization; writing – review and editing; project administration; supervision. **Neville H. McClenaghan:** Conceptualization; project administration; supervision; writing – review and editing.

### ACKNOWLEDGMENTS

We acknowledged the financial support in the Funding Information section.

### FUNDING INFORMATION

These studies were supported in part by the Research and Development Office of the Northern Ireland Department for Health and Personal Social Services and University of Ulster Research strategy funding. RCM is recipient of the RD Lawrence Fellowship from Diabetes UK.

### CONFLICT OF INTEREST STATEMENT

All authors declare no conflicts of interest.

### DATA AVAILABILITY STATEMENT


The data that support the findings of this study are available from the corresponding author upon reasonable request.

### ORCID

R. Charlotte Moffett  <https://orcid.org/0000-0002-7196-7863>

Lorraine Brennan  <https://orcid.org/0000-0002-7711-7499>

Peter R. Flatt  <https://orcid.org/0000-0001-8548-7943>

Neville H. McClenaghan  <https://orcid.org/0000-0001-5412-0241>

Andrei I. Tarasov  <https://orcid.org/0000-0002-8883-176X>

### REFERENCES

- Malaisse W. Insulin release: the fuel concept. *Diabète Métab.* 1983;9(4):313-320.
- Henquin J-C. Regulation of insulin release by ionic and electrical events in B cells. *Horm Res Paediatr.* 1987;27(3):168-178.
- Hellman B, Sehlin J, Täljedal I-B. Effects of glucose and other modifiers of insulin release on the oxidative metabolism of amino acids in micro-dissected pancreatic islets. *Biochem J.* 1971;123(4):513-521.
- Newsholme P, Brennan L, Bender K. Amino acid metabolism,  $\beta$ -cell function, and diabetes. *Diabetes.* 2006;55(Supplement\_2):S39-S47.
- Han G, Takahashi H, Murao N, et al. Glutamate is an essential mediator in glutamine-amplified insulin secretion. *J Diabetes Invest.* 2021;12(6):920-930.
- Helman A, Cangelosi AL, Davis JC, et al. A nutrient-sensing transition at birth triggers glucose-responsive insulin secretion. *Cell Metab.* 2020;31(5):1004-1016. e1005.
- Maechler P, Wollheim CB. Mitochondrial signals in glucose-stimulated insulin secretion in the beta cell. *J Physiol.* 2000;529(1):49-56.
- Turbitt J, Brennan L, Moffett RC, et al. NKCC transport mediates the insulinotropic effects of taurine and other small neutral amino acids. *Life Sci.* 2023;316:121402.
- Sarnobat D, Moffett RC, Ma J, Flatt PR, McClenaghan NH, Tarasov AI. Taurine rescues pancreatic  $\beta$ -cell stress by stimulating  $\alpha$ -cell transdifferentiation. *BioFactors.* 2023;49:646-662.
- Carneiro EM, Latorraca MQ, Araujo E, et al. Taurine supplementation modulates glucose homeostasis and islet function. *J Nutr Biochem.* 2009;20(7):503-511.
- Cherif H, Reusens B, Ahn M, Hoet J, Remacle C. Effects of taurine on the insulin secretion of rat fetal islets from dams fed a low-protein diet. *J Endocrinol.* 1998;159(2):341-348.
- Kulakowski EC, Maturio J. Hypoglycemic properties of taurine: not mediated by enhanced insulin release. *Biochem Pharmacol.* 1984;33(18):2835-2838.
- Bustamante J, Alonso FJ, Lobo MV, et al. Taurine levels and localization in pancreatic islets. *Taurine 3.* Springer; 1998:65-69.
- Yahara T, Tachikawa M, Akanuma S-i, Kubo Y, Hosoya K-i. Amino acid residues involved in the substrate specificity of TauT/SLC6A6 for taurine and  $\gamma$ -aminobutyric acid. *Biol Pharm Bull.* 2014;37(5):817-825.
- Tarasov A, Dusonchet J, Ashcroft F. Metabolic regulation of the pancreatic beta-cell ATP-sensitive K<sup>+</sup> channel: a pas de deux. *Diabetes.* 2004;53(Suppl 3):S113-S122.
- MacDonald MJ, Fahien LA, Brown LJ, Hasan NM, Buss JD, Kendrick MA. Perspective: emerging evidence for signaling

- roles of mitochondrial anaplerotic products in insulin secretion. *Am J Physiol Endocrinol Metab.* 2005;288(1):E1-E15.
17. Henquin J-C. Triggering and amplifying pathways of regulation of insulin secretion by glucose. *Diabetes.* 2000;49(11):1751-1760.
  18. Gunawardana SC, Liu Y-J, MacDonald MJ, Straub SG, Sharp GW. Anaplerotic input is sufficient to induce time-dependent potentiation of insulin release in rat pancreatic islets. *Am J Physiol Endocrinol Metab.* 2004;287(5):E828-E833.
  19. Tarasov AI, Galvanovskis J, Rorsman O, et al. Monitoring real-time hormone release kinetics via high-content 3-D imaging of compensatory endocytosis. *Lab Chip.* 2018;18(18):2838-2848.
  20. Hamilton A, Vergari E, Miranda C, Tarasov AI. Imaging calcium dynamics in subpopulations of mouse pancreatic islet cells. *JoVE (J Vis Exp).* 2019;153:e59491.
  21. Berg J, Hung YP, Yellen G. A genetically encoded fluorescent reporter of ATP:ADP ratio. *Nat Methods.* 2009;6(2):161-166.
  22. Koberstein JN, Stewart ML, Smith CB, et al. Monitoring glycolytic dynamics in single cells using a fluorescent biosensor for fructose 1, 6-bisphosphate. *Proc Natl Acad Sci USA.* 2022;119(31):e2204407119.
  23. Lake SP, Bassett PD, Larkins A, et al. Large-scale purification of human islets utilizing discontinuous albumin gradient on IBM 2991 cell separator. *Diabetes.* 1989;38(Suppl 1):143-145.
  24. Ricordi C, Lacy PE, Finke EH, Olack BJ, Scharp DW. Automated method for isolation of human pancreatic islets. *Diabetes.* 1988;37(4):413-420.
  25. Tarasov AI, Rutter GA. Use of genetically encoded sensors to monitor cytosolic ATP/ADP ratio in living cells. *Methods Enzymol.* 2014;542:289-311.
  26. McClenaghan NH, Barnett CR, Ah-Sing E, et al. Characterization of a novel glucose-responsive insulin-secreting cell line, BRIN-BD11, produced by electrofusion. *Diabetes.* 1996;45(8):1132-1140.
  27. Kelly C, Flatt PR, McClenaghan NH. Cell-to-cell communication and cellular environment alter the somatostatin status of delta cells. *Biochem Biophys Res Commun.* 2010;399(2):162-166.
  28. Pettengill OS, Memoli VA, Brinck-Johnsen T, Longnecker DS. Cell lines derived from pancreatic tumors of Tg (Ela-1-SV40E) Bri18 transgenic mice express somatostatin and antigen. *Carcinogenesis.* 1994;15(1):61-65.
  29. Henquin J-C, Nenquin M, Stiernet P, Ahren B. In vivo and in vitro glucose-induced biphasic insulin secretion in the mouse: pattern and role of cytoplasmic  $Ca^{2+}$  and amplification signals in  $\beta$ -cells. *Diabetes.* 2006;55(2):441-451.
  30. Flatt P, Bailey C. Abnormal plasma glucose and insulin responses in heterozygous lean (ob/+) mice. *Diabetologia.* 1981;20(5):573-577.
  31. Miguel JC, Patterson S, Abdel-Wahab YH, Mathias PC, Flatt PR. Time-correlation between membrane depolarization and intracellular calcium in insulin secreting BRIN-BD11 cells: studies using FLIPR. *Cell Calcium.* 2004;36(1):43-50.
  32. R Development Core Team. *R: A Language and Environment for Statistical Computing, Vienna, Austria* 2016; Accessed April 2018. <https://www.R-project.org/>
  33. Marselli L, Thorne J, Dahiya S, et al. Gene expression profiles of Beta-cell enriched tissue obtained by laser capture microdissection from subjects with type 2 diabetes. *PloS One.* 2010;5(7):e11499.
  34. Russ HA, Sintov E, Anker-Kitai L, et al. Insulin-producing cells generated from dedifferentiated human pancreatic beta cells expanded in vitro. *PloS One.* 2011;6(9):e25566.
  35. DiGrucchio MR, Mawla AM, Donaldson CJ, et al. Comprehensive alpha, beta and delta cell transcriptomes reveal that ghrelin selectively activates delta cells and promotes somatostatin release from pancreatic islets. *Mol Metab.* 2016;5(7):449-458.
  36. Adriaenssens AE, Svendsen B, Lam BY, et al. Transcriptomic profiling of pancreatic alpha, beta and delta cell populations identifies delta cells as a principal target for ghrelin in mouse islets. *Diabetologia.* 2016;59(10):2156-2165.
  37. Xu YX, Wagenfeld A, Yeung CH, Lehnert W, Cooper T. Expression and location of taurine transporters and channels in the epididymis of infertile c-ros receptor tyrosine kinase-deficient and fertile heterozygous mice. *Mol Reprod Dev.* 2003;64(2):144-151.
  38. Richter M, Moroniak SJ, Michel H. Identification of competitive inhibitors of the human taurine transporter TauT in a human kidney cell line. *Pharmacol Rep.* 2019;71(1):121-129.
  39. Bustamante J, Lobo M, Alonso F, et al. An osmotic-sensitive taurine pool is localized in rat pancreatic islet cells containing glucagon and somatostatin. *Am J Physiol Endocrinol Metab.* 2001;281(6):E1275-E1285.
  40. Prentki M, Renold A. Neutral amino acid transport in isolated rat pancreatic islets. *J Biol Chem.* 1983;258(23):14239-14244.
  41. L'Amoreaux WJ, Cuttitta C, Santora A, Blaize JF, Tachjadi J, El Idrissi A. Taurine regulates insulin release from pancreatic beta cell lines. *J Biomed Sci.* 2010;17(1):1-8.
  42. Dabrowski M, Tarasov A, Ashcroft FM. Mapping the architecture of the ATP-binding site of the KATP channel subunit Kir6.2. *J Physiol.* 2004;557(2):347-354.
  43. Baliou S, Kyriakopoulos AM, Goulielmaki M, Panayiotidis MI, Spandidos DA, Zoumpourlis V. Significance of taurine transporter (TauT) in homeostasis and its layers of regulation. *Mol Med Rep.* 2020;22(3):2163-2173.
  44. GTEx Consortium, Ardlie KG, Deluca DS, Segrè AV, et al. The genotype-tissue expression (GTEx) pilot analysis: multitissue gene regulation in humans. *Science.* 2015;348(6235):648-660.
  45. Uhlén M, Fagerberg L, Hallström BM, et al. Tissue-based map of the human proteome. *Science.* 2015;347(6220):1260419.
  46. Fagerberg L, Hallström BM, Oksvold P, et al. Analysis of the human tissue-specific expression by genome-wide integration of transcriptomics and antibody-based proteomics. *Mol Cell Proteom.* 2014;13(2):397-406.
  47. Han X, Patters AB, Chesney RW. Gating of taurine transport: role of the fourth segment of the taurine transporter. *Taurine 5: Beginning the 21st Century*; London/New York: Kluwer Academic/Plenum. 2003:149-157.
  48. Han X, Patters A, Jones D, Zelikovic I, Chesney R. The taurine transporter: mechanisms of regulation. *Acta Physiol.* 2006;187(1-2):61-73.
  49. Qu F, ElOmari K, Wagner A, De Simone A, Beis K. Desolvation of the substrate-binding protein TauA dictates ligand specificity for the alkanesulfonate ABC importer TauABC. *Biochem J.* 2019;476(23):3649-3660.
  50. Komatsu M, Schermerhorn T, Aizawa T, Sharp GW. Glucose stimulation of insulin release in the absence of extracellular  $Ca^{2+}$  and in the absence of any increase in intracellular  $Ca^{2+}$  in rat pancreatic islets. *Proc Natl Acad Sci USA.* 1995;92(23):10728-10732.

51. Sato Y, Nenquin M, Henquin JC. Relative contribution of  $\text{Ca}^{2+}$ -dependent and  $\text{Ca}^{2+}$ -independent mechanisms to the regulation of insulin secretion by glucose. *FEBS Lett*. 1998;421(2):115-119.
52. Tarasov AI, Welters HJ, Senkel S, et al. A Kir6.2 mutation causing neonatal diabetes impairs electrical activity and insulin secretion from INS-1 beta-cells. *Diabetes*. 2006;55(11):3075-3082.
53. Sluga N, Križančić Bombek L, Kerčmar J, et al. Physiological levels of adrenaline fail to stop pancreatic beta cell activity at unphysiologically high glucose levels. *Front Endocrinol*. 2022;2686:1013697.
54. Eliasson L, Renström E, Ding WG, Proks P, Rorsman P. Rapid ATP-dependent priming of secretory granules precedes  $\text{Ca}^{2+}$ -induced exocytosis in mouse pancreatic B-cells. *J Physiol*. 1997;503(2):399-412.
55. Hagan DW, Ferreira SM, Santos GJ, Phelps EA. The role of GABA in islet function. *Front Endocrinol*. 2022;13:972115.
56. De Luca A, Pierno S, Camerino DC. Taurine: the appeal of a safe amino acid for skeletal muscle disorders. *J Transl Med*. 2015;13(1):1-18.
57. Vinton NE, Laidlaw SA, Ament ME, Kopple JD. Taurine concentrations in plasma, blood cells, and urine of children undergoing long-term total parenteral nutrition. *Pediatr Res*. 1987;21(4):399-403.
58. Ghandforoush-Sattari M, Mashayekhi S, Krishna CV, Thompson JP, Routledge PA. Pharmacokinetics of oral taurine in healthy volunteers. *J Amino Acids*. 2010;2010:1-5.
59. Lavine JA, Kibbe CR, Baan M, et al. Cholecystokinin expression in the  $\beta$ -cell leads to increased  $\beta$ -cell area in aged mice and protects from streptozotocin-induced diabetes and apoptosis. *Am J Physiol Endocrinol Metab*. 2015;309(10):E819-E828.
60. Tarasov AI, Semplici F, Li D, et al. Frequency-dependent mitochondrial  $\text{Ca}^{2+}$  accumulation regulates ATP synthesis in pancreatic  $\beta$  cells. *Pflug Arch Eur J Physiol*. 2013;465(4):543-554.
61. Mobbs JJ, Belousoff MJ, Harikumar KG, et al. Structures of the human cholecystokinin 1 (CCK1) receptor bound to Gs and Gq mimetic proteins provide insight into mechanisms of G protein selectivity. *PLoS Biol*. 2021;19(6):e3001295.
62. Tengholm A, Gylfe E. cAMP signalling in insulin and glucagon secretion. *Diabetes Obes Metab*. 2017;19:42-53.
63. Farilla L, Bulotta A, Hirshberg B, et al. Glucagon-like peptide 1 inhibits cell apoptosis and improves glucose responsiveness of freshly isolated human islets. *Endocrinology*. 2003;144(12):5149-5158.
64. Gaus B, Brüning D, Hatlapatka K, Rustenbeck I. Changes in granule mobility and age contribute to changes in insulin secretion after desensitization or rest. *BMJ Open Diabetes Res Care*. 2021;9(1):e002394.
65. Stancill JS, Cartiailler J-P, Clayton HW, et al. Chronic  $\beta$ -cell depolarization impairs  $\beta$ -cell identity by disrupting a network of  $\text{Ca}^{2+}$ -regulated genes. *Diabetes*. 2017;66(8):2175-2187.
66. Osipovich AB, Stancill JS, Cartiailler J-P, Dudek KD, Magnuson MA. Excitotoxicity and overnutrition additively impair metabolic function and identity of pancreatic  $\beta$ -cells. *Diabetes*. 2020;69(7):1476-1491.
67. Shigeto M, Ramracheya R, Tarasov AI, et al. GLP-1 stimulates insulin secretion by PKC-dependent TRPM4 and TRPM5 activation. *J Clin Investig*. 2015;125(12):4714-4728.
68. Liu Q-R, Lopez-Corcuera B, Nelson H, Mandiyan S, Nelson N. Cloning and expression of a cDNA encoding the transporter of taurine and beta-alanine in mouse brain. *Proc Natl Acad Sci USA*. 1992;89(24):12145-12149.

## SUPPORTING INFORMATION

Additional supporting information can be found online in the Supporting Information section at the end of this article.

**How to cite this article:** Turbitt J, Moffett RC, Brennan L, et al. Molecular determinants and intracellular targets of taurine signalling in pancreatic islet  $\beta$ -cells. *Acta Physiol*. 2024;00:e14101. doi:[10.1111/apha.14101](https://doi.org/10.1111/apha.14101)